Supporting Information

Synthesis and reactivities of polyhydrido osmium arylsilyl complexes prepared from $OsH_3Cl(PPh_3)_3$

Guomei He,[†,‡] Linlin Wu,[†] Wei Bai,[†] Jiangxi Chen,*[,‡] Herman H. Y. Sung,[†] Ian D. Williams,[†] Zhenyang Lin*[,†] and Guochen Jia*[,†]

†. Department of Chemistry, The Hong Kong University of Science and Technology, Clear Water Bay, Kowloon, Hong Kong.

‡. Department of Materials Science and Engineering, College of Materials, Xiamen University, Xiamen, China.

Table of Contents

1. Spectroscopic data

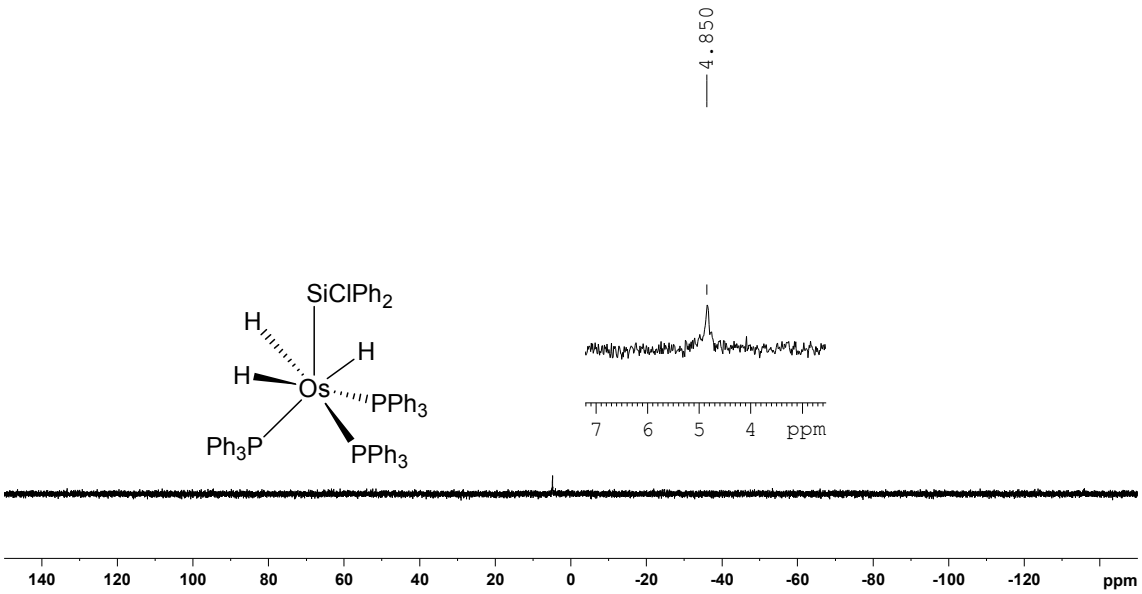

Figure S1. The $^{31}P\{^{1}H\}$ NMR spectrum of **2** in CD_2Cl_2 at 161.98 MHz.

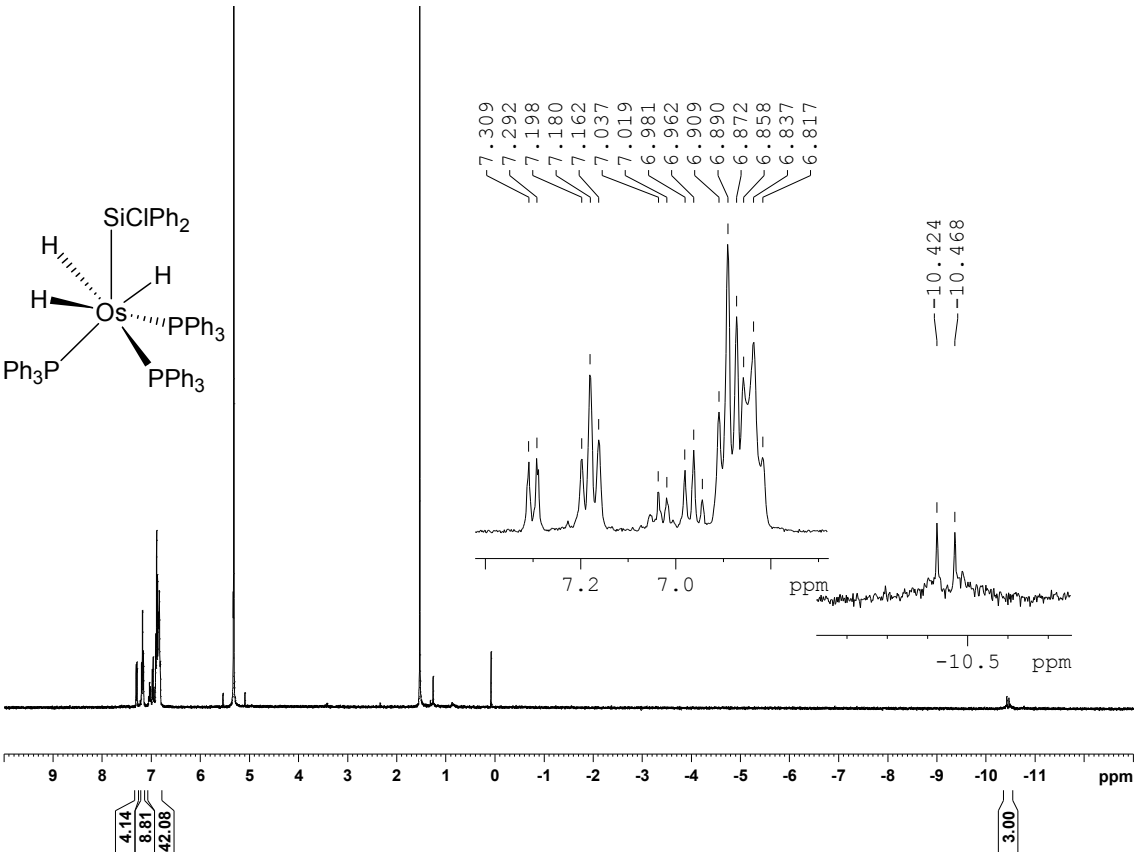

Figure S2. The ^{1}H NMR spectrum of **2** in CD_2Cl_2 at 400.13 MHz.

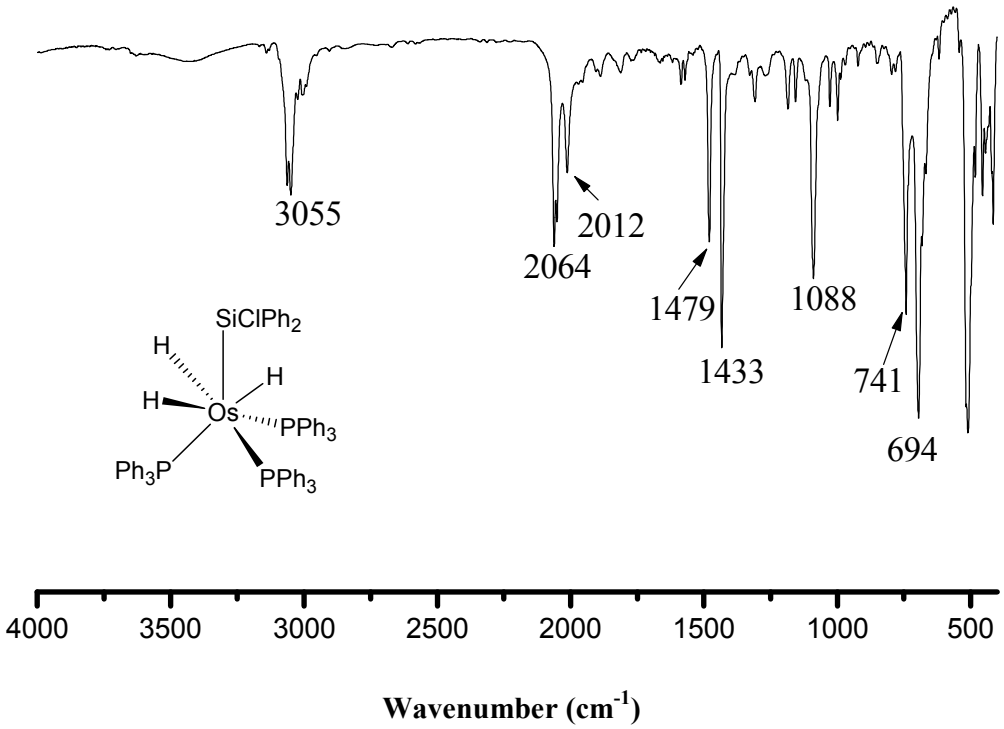

Figure S3. The IR spectrum of **2.**

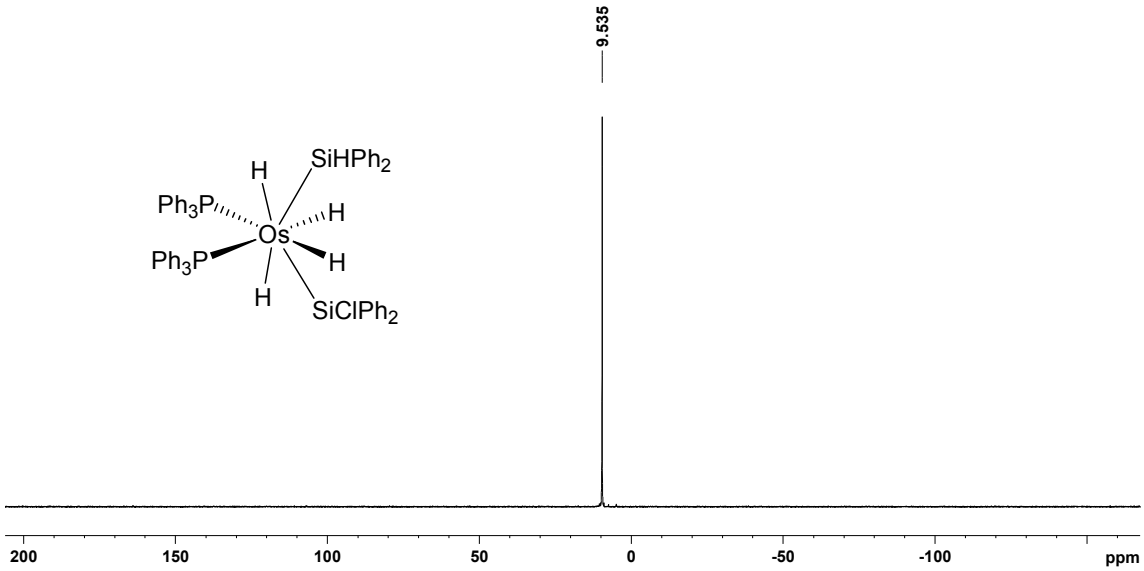

Figure S4. The $^{31}P\{^{1}H\}$ NMR spectrum of **3** in C_6D_6 at 121.49 MHz.

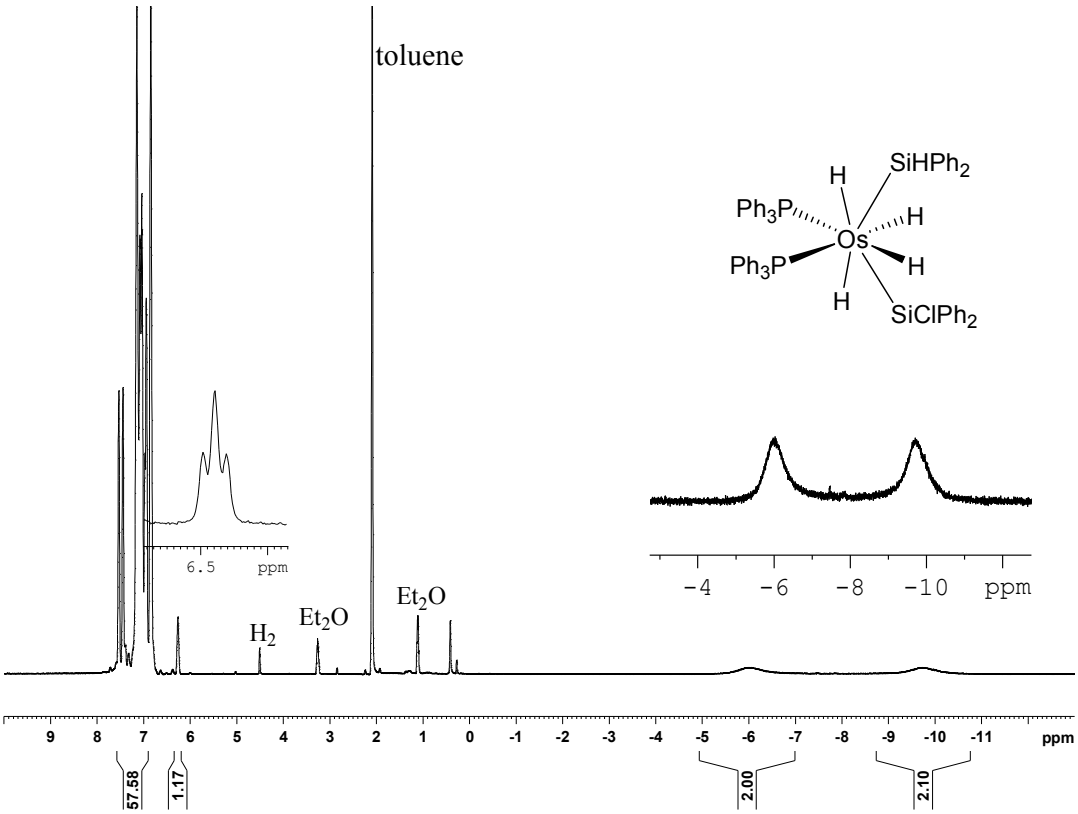

Figure S5. The ^{1}H NMR spectrum of **3** in $C_6D_5CD_3$ at 400.13 MHz.

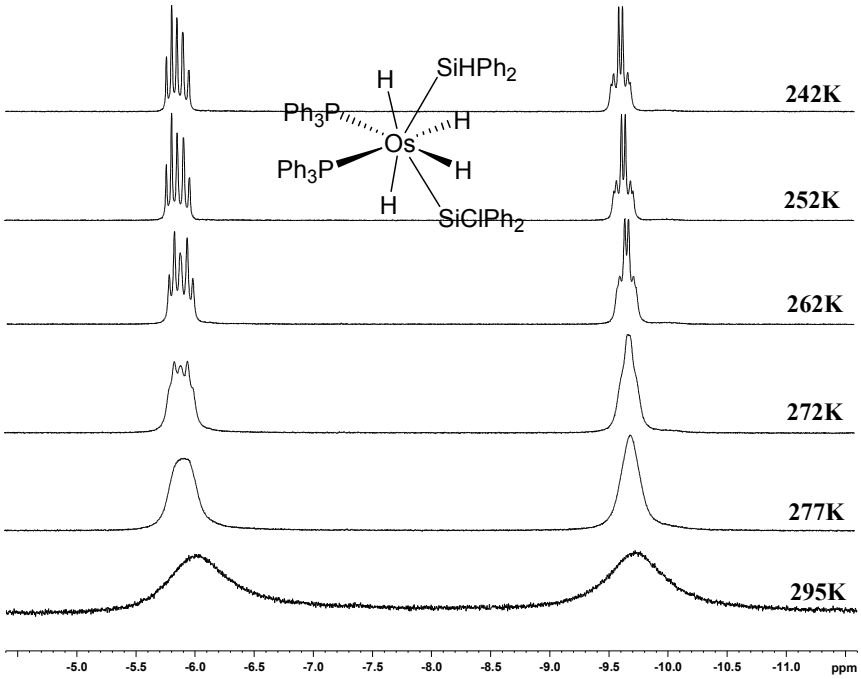

Figure S6. The hydride region ^{1}H NMR spectra of **3** in $C_6D_5CD_3$ at various temperatures.

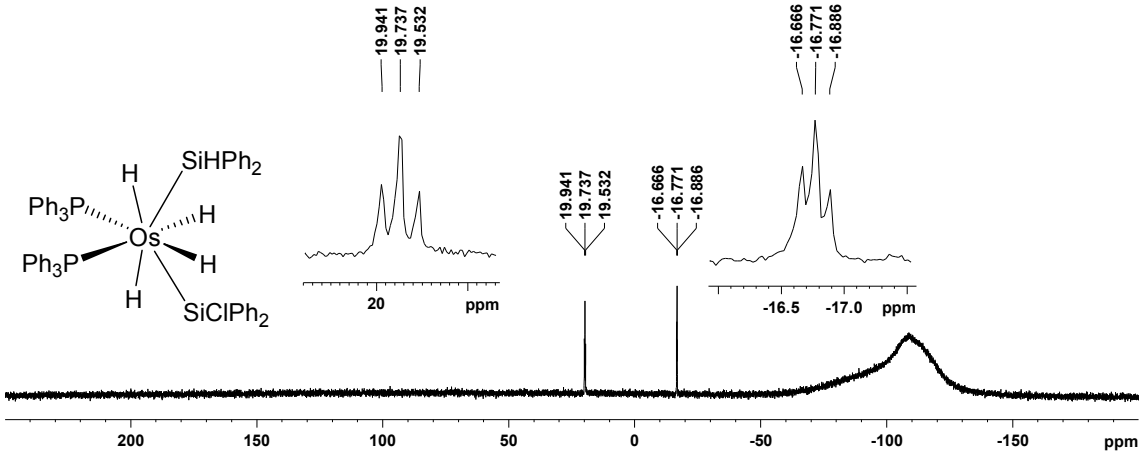

Figure S7. The $^{29}Si\{^{1}H\}$ NMR spectrum of **3** in C_6D_6 at 59.63 MHz.

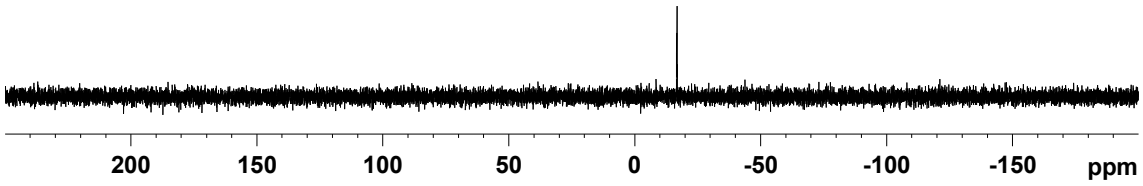

Figure S8. The ^{29}Si DEPT135 NMR spectrum of **3** in C_6D_6 at 59.63 MHz.

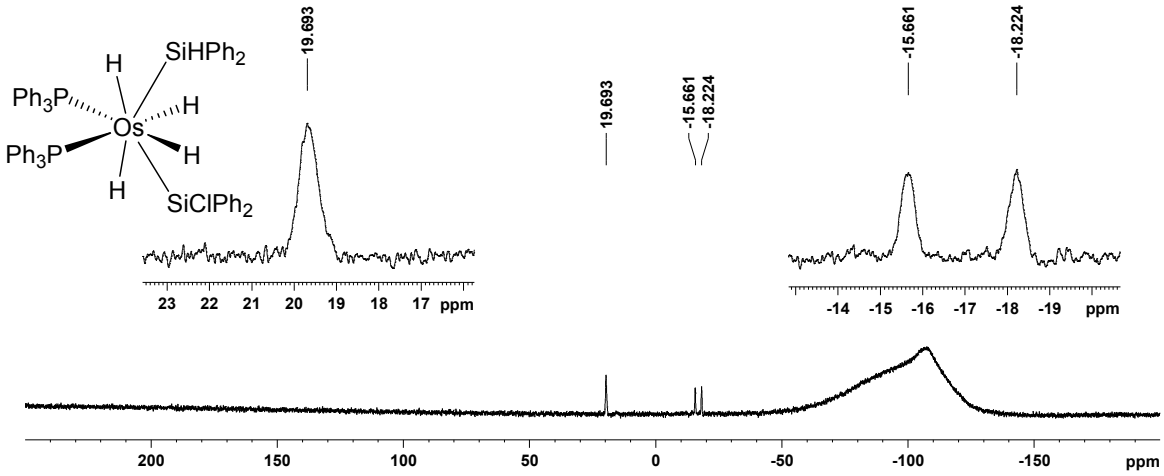

Figure S9. The ^{29}Si NMR spectrum of **3** in $C_6D_5CD_3$ at 79.49 MHz.

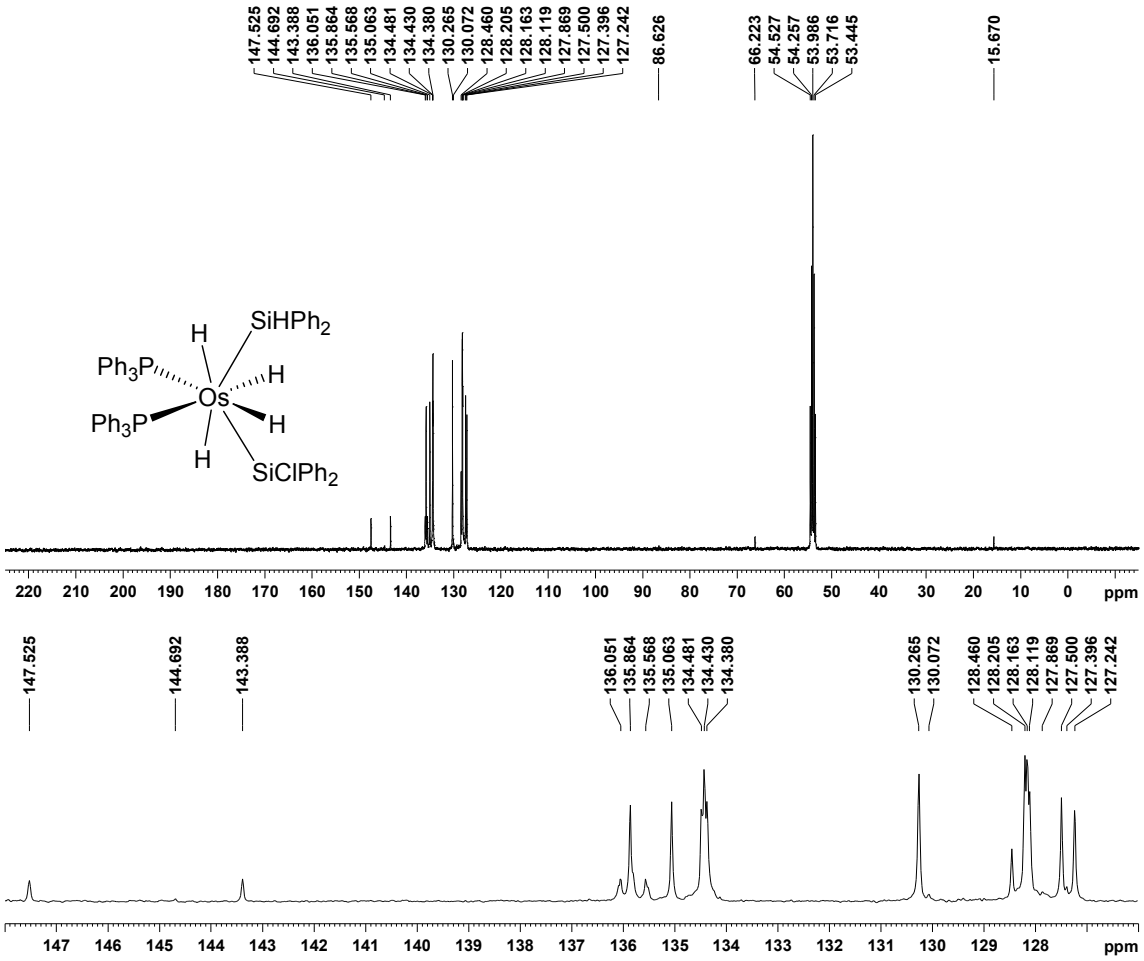

Figure S10. The $^{13}C\{^{1}H\}$ NMR spectrum of **3** in CD_2Cl_2 at 100.62MHz.

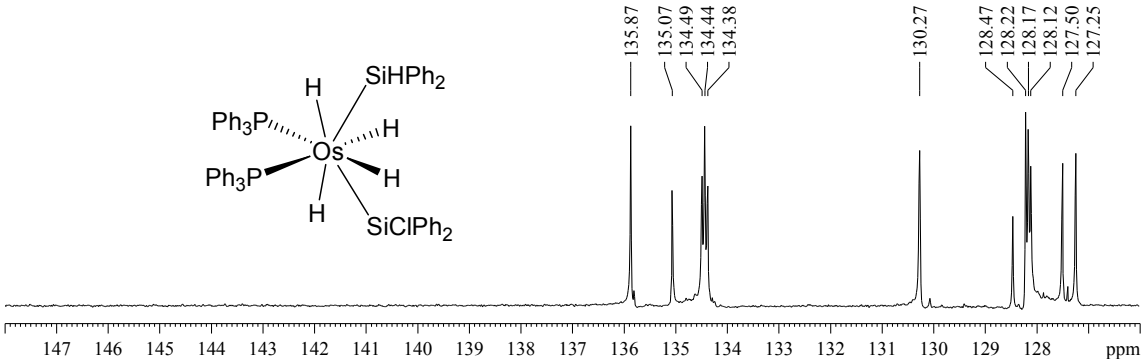

Figure S11. The ^{13}C DEPT135 NMR spectrum of **3** in CD_2Cl_2 at 100.62MHz.

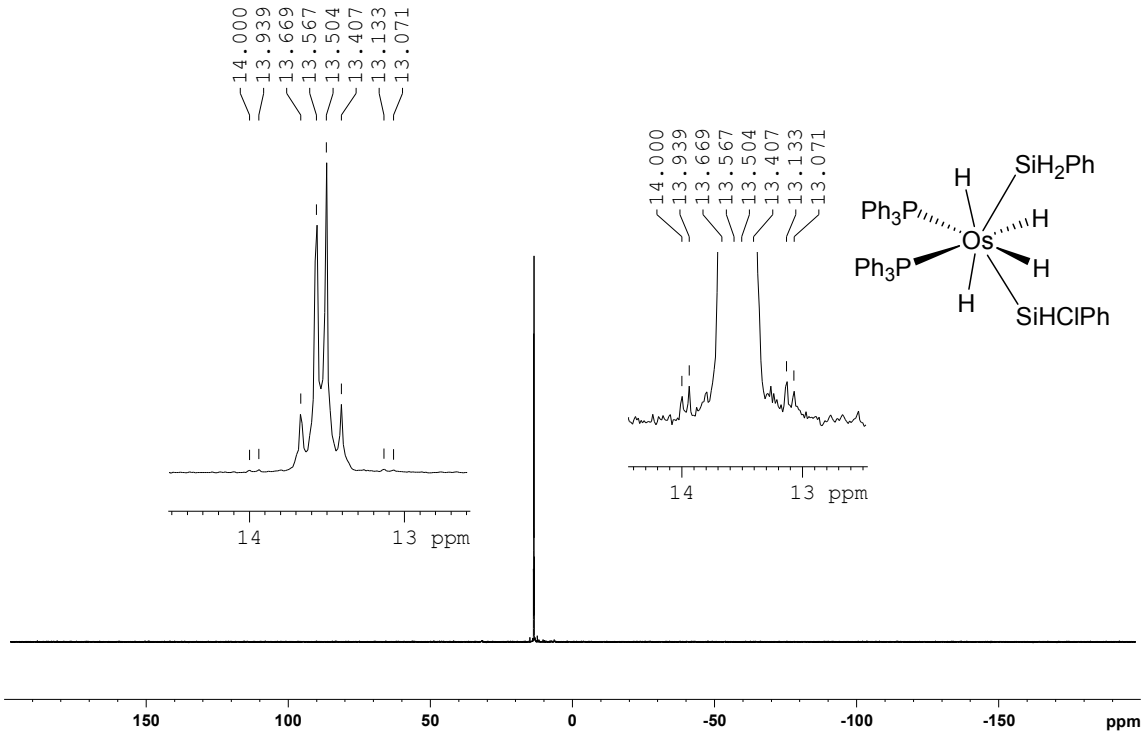

Figure S12. The $^{31}P\{^{1}H\}$ NMR spectrum of **4** in C_6D_6 at 161.98 MHz.

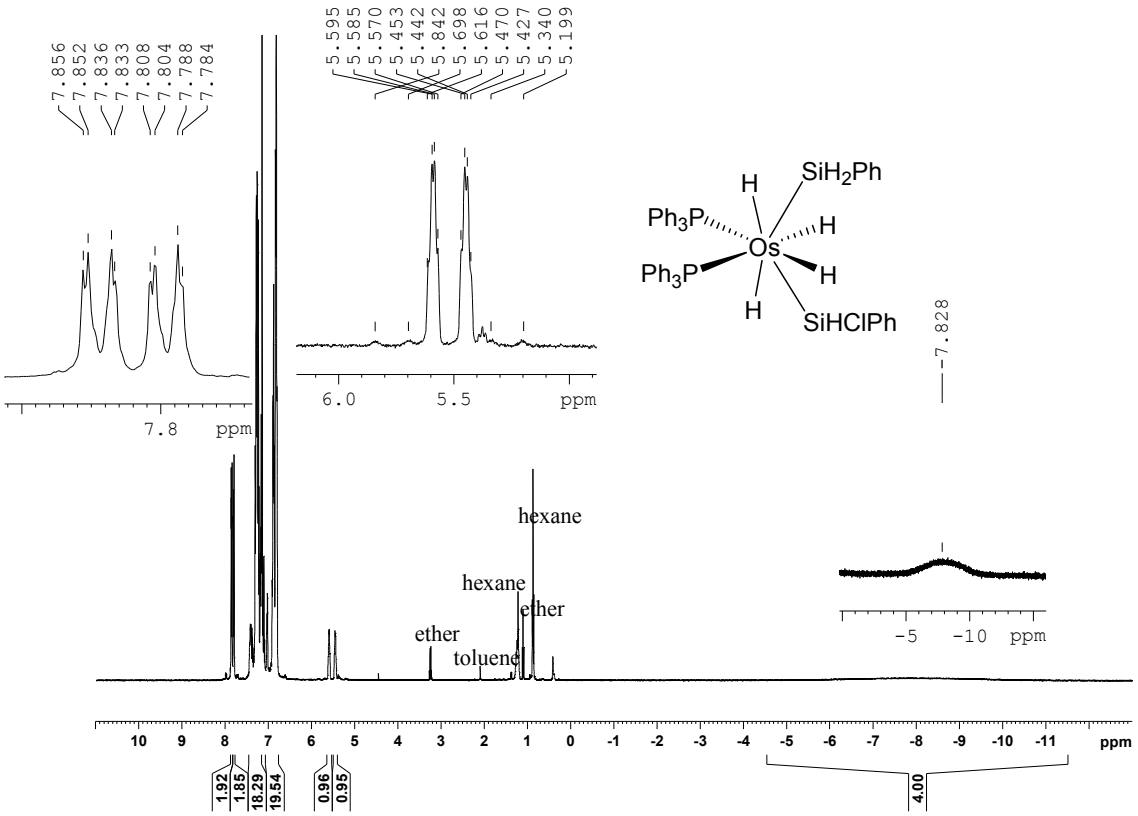

Figure S13. The ^{1}H NMR spectrum of **4** in C_6D_6 at 400.13 MHz.

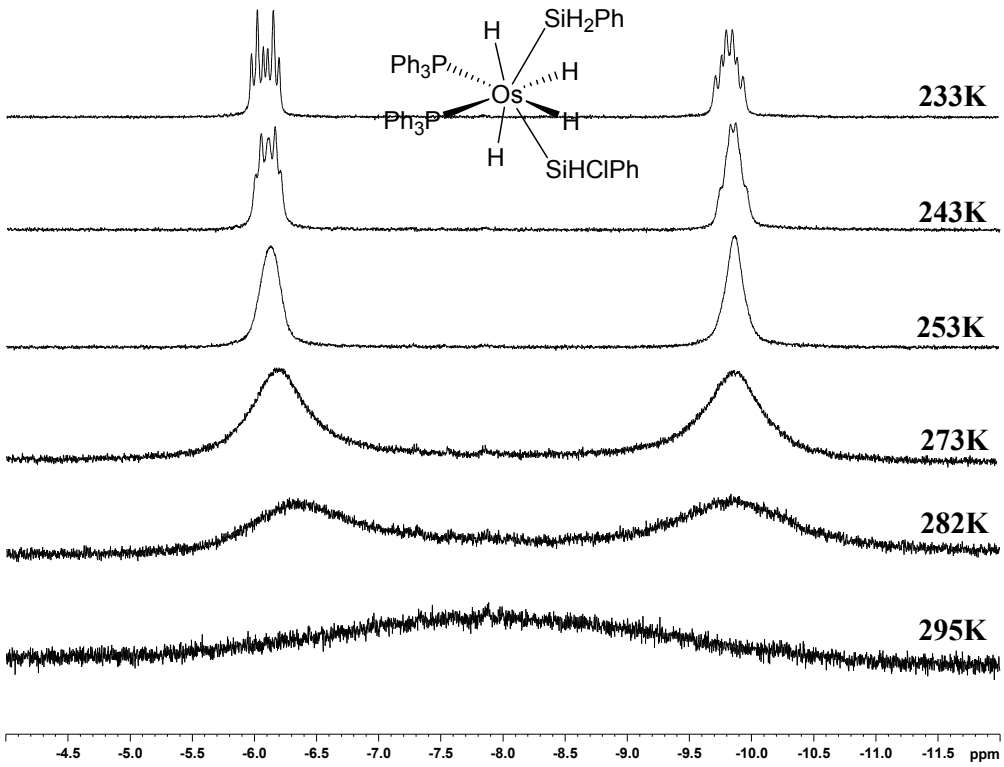

Figure S14. The ^{1}H NMR spectra of **4** in $C_6D_5CD_3$ at various temperatures.

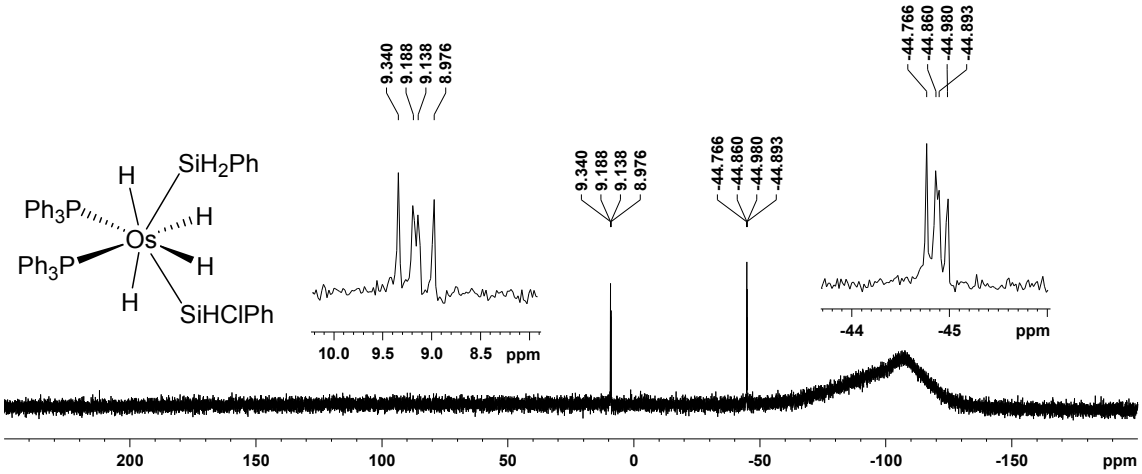

Figure S15. The ^{29}Si{^{1}H} NMR spectrum of **4** in C_6D_6 at 59.63 MHz.

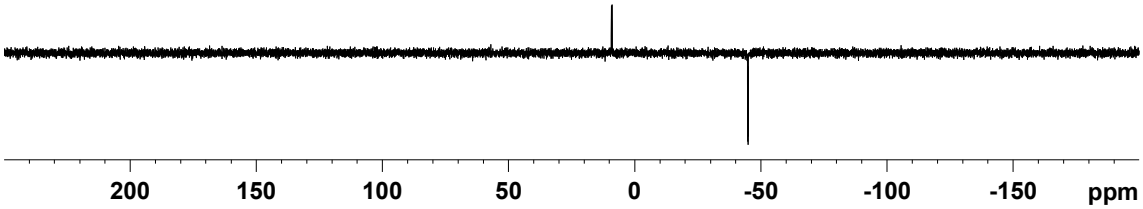

Figure S16. The ^{29}Si DEPT135 NMR spectrum of **4** in C_6D_6 at 59.63 MHz.

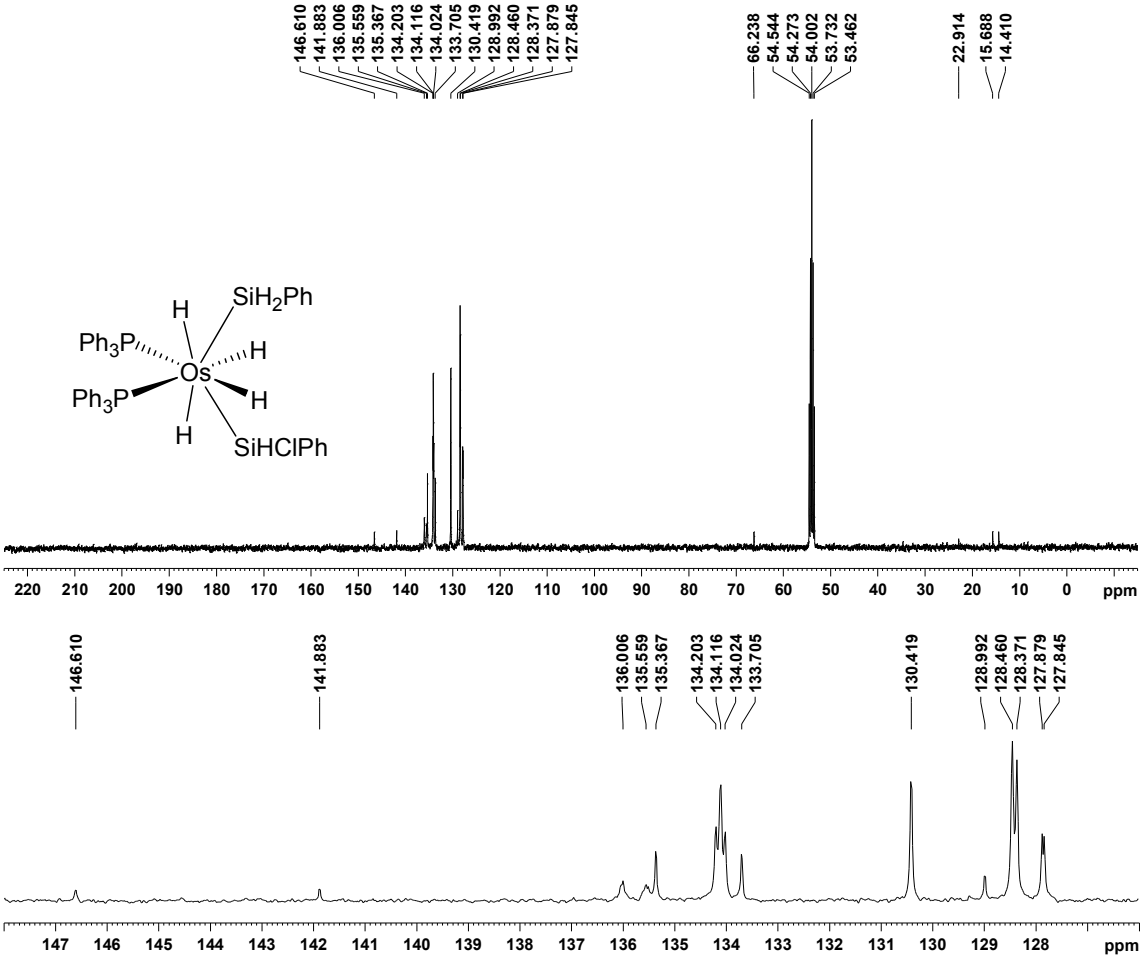

Figure S17. The $^{13}C\{^1H\}$ NMR spectrum of **4** in CD_2Cl_2 at 100.62 MHz.

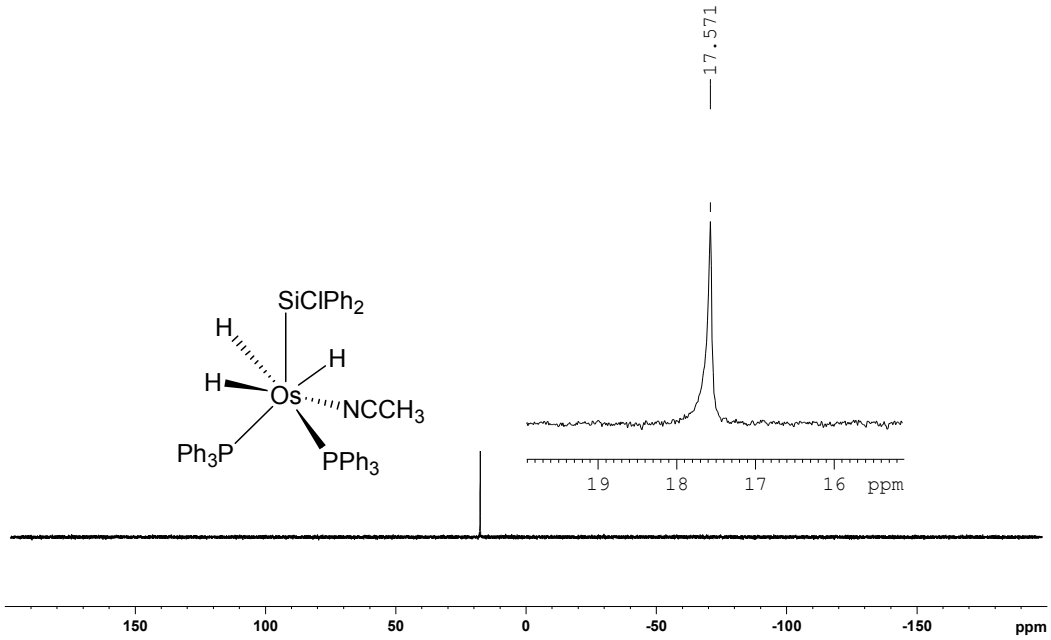

Figure S18. The $^{31}P\{^{1}H\}$ NMR spectrum of **18** in C_6D_6 at 161.98 MHz.

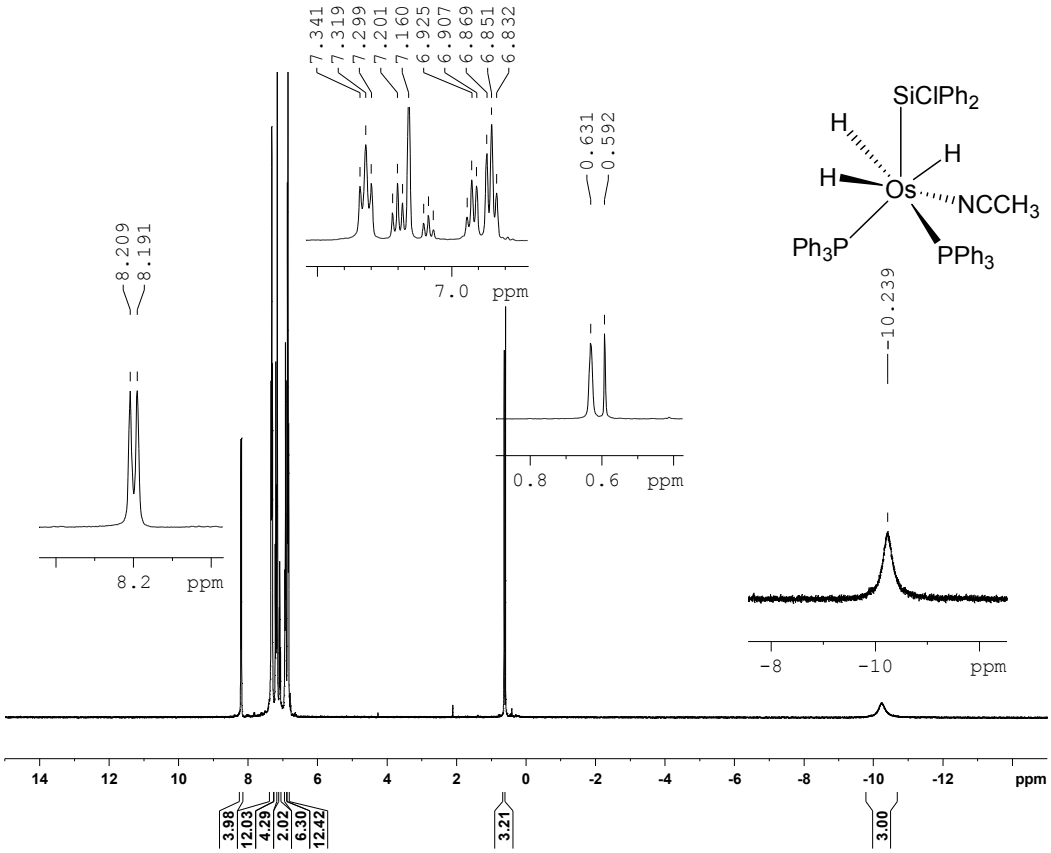

Figure S19. The ^{1}H NMR spectrum of **18** in C_6D_6 at 400.13 MHz.

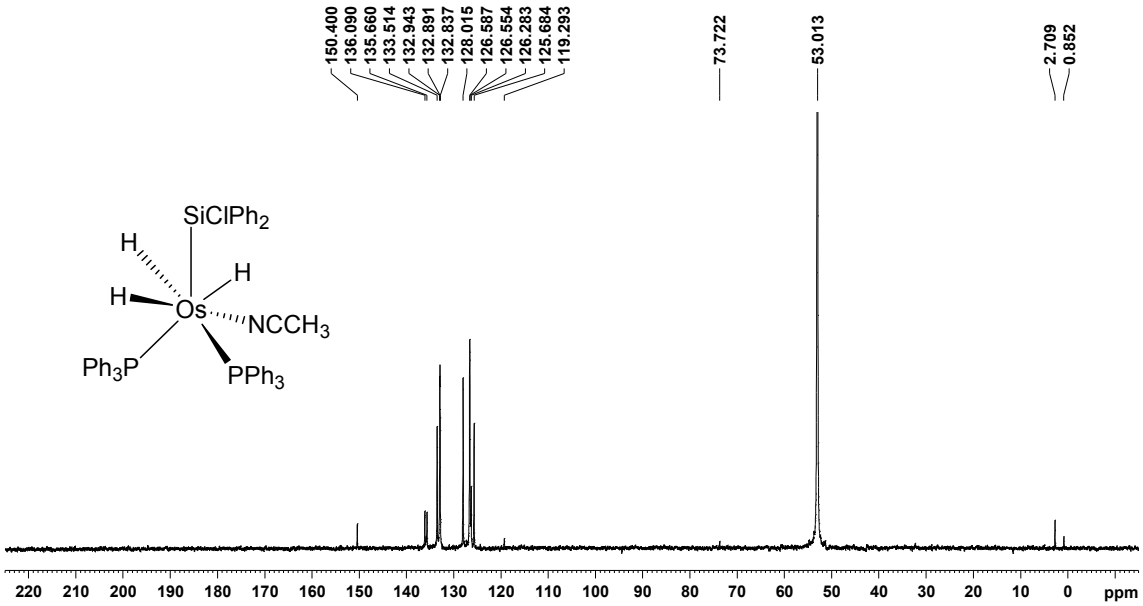

Figure S20. The $^{13}C\{^{1}H\}$ NMR of **18** in C_6D_6 at 100.62 MHz.

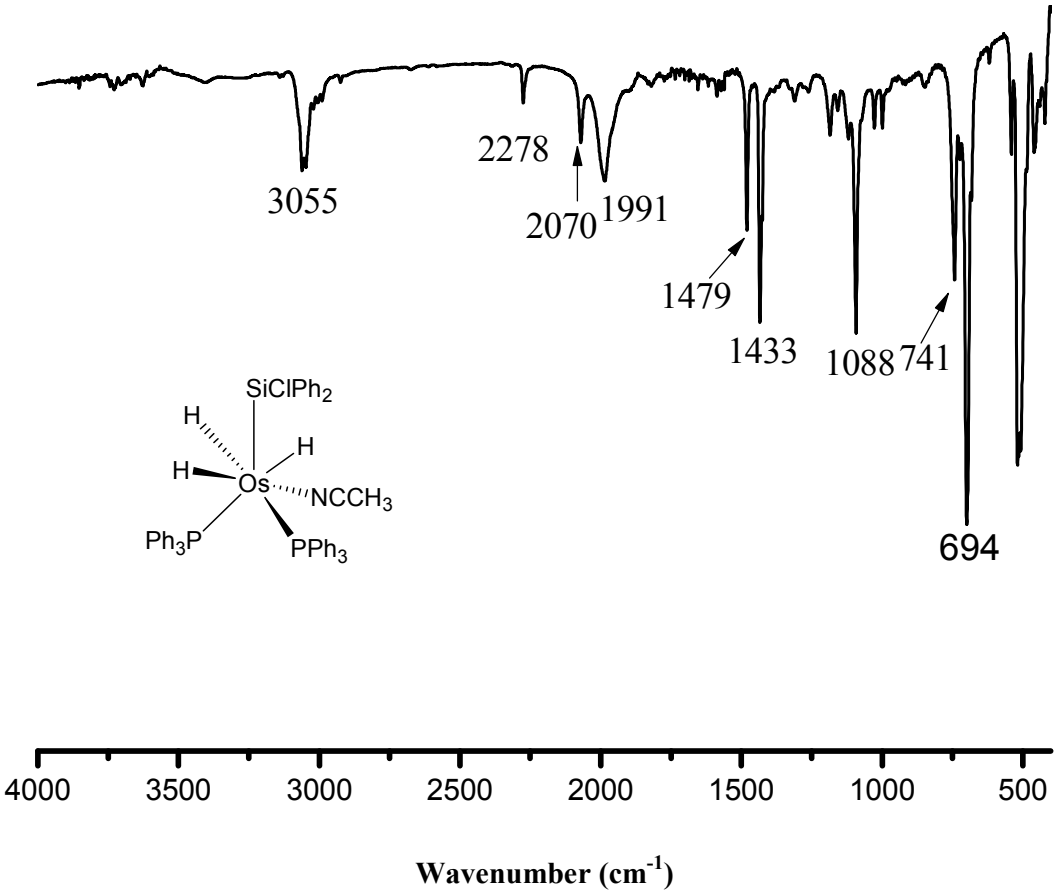

Figure S21. The IR spectrum of **18.**

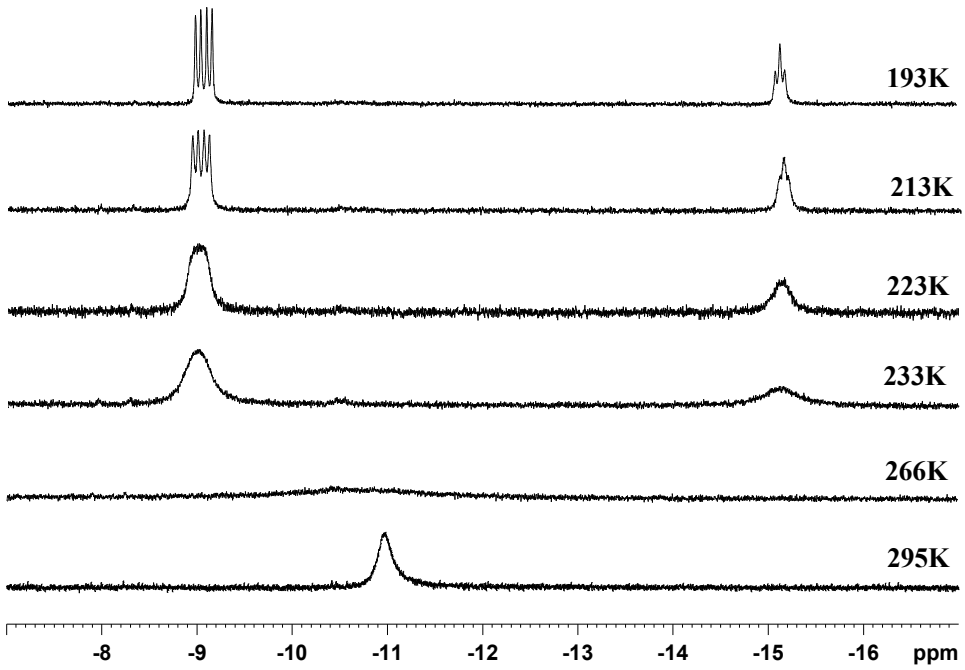

Figure S22. The hydride region of the ^{1}H NMR spectra of **18** in CD_2Cl_2 at 295-193 K.

2. Crystallographic details for complexes 3 and 18.

Table S1. Crystallographic details for complexes **3** and **18**.

Identification code	**3**	**18**·CH_2Cl_2
Empirical formula	$C_{60}H_{55}ClOsP_2Si_2$	$C_{51}H_{48}Cl_3NOsP_2Si$
Formula weight	1119.81	1061.48
Temperature, K	99.98(10)	100.00(10)
Wavelength, Å	1.54184	1.54184
Crystal system	Orthorhombic	Triclinic
Space group	$P2_12_12_1$	P-1
a, Å	12.3673(3)	9.2081(3)
b, Å	15.5428(4)	12.9942(3)
c, Å	26.5491(8)	19.8346(5)
α, deg.	90	83.214(2)
β, deg.	90	82.790(2)
γ, deg.	90	73.209(2)
Volume, $Å^3$	5103.3(2)	2245.68(11)
Z	4	2
d (calculated), Mg/m^3	1.457	1.570
Two Theta range for data collection, deg.	7.886 to 133.992	8.764 to 133.994
Reflections collected	28522	12759
Independent reflections	9052 [R(int) = 0.0682]	7855 [R(int) = 0.0168]
Data / restraints / parameters	9052/57/610	7855/0/545
Goodness-of-fit on F^2	1.002	1.000
Final R indices [I>2sigma(I)]	R_1 = 0.0409, wR_2 = 0.0911	R1 = 0.0165, wR2 = 0.0397
Largest diff. peak / hole, $e.Å^{-3}$	0.91/-0.62	0.74/-0.76

3. Optimized structures

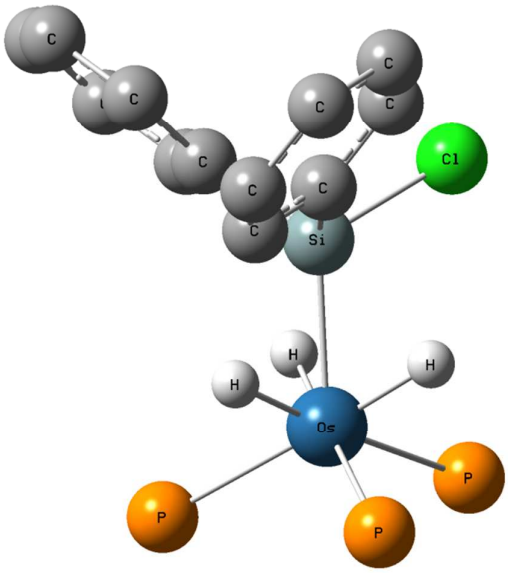

Os-P1 = 2.53316
Os-P2 = 2.53242
Os-P3 = 2.49149
Os-Si = 2.38023

Os-H1 = 1.63427
Os-H2 = 1.63633
Os-H3 = 1.64629

Cl-Si = 2.16281
Si-H1 = 2.12783
Si-H2 = 2.19268
Si-H3 = 2.21649

H1-H2 = 2.55427
H2-H3 = 2.48380
H1-H3 = 2.51066

P1-Os-P2 = 105.95618
Si-Os-P1 = 117.26086
Si-Os-P2 = 114.68855
Si-Os-P3 = 112.18232
P2-Os-P3 = 101.76370
P3-Os-P1 = 103.28435
H1-Os-P1 = 177.93324
H2-Os-P2 = 177.68403
H3-Os-P3 = 175.95804

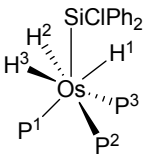

2

Figure S23. B3LYP optimized structure of complex **2**.

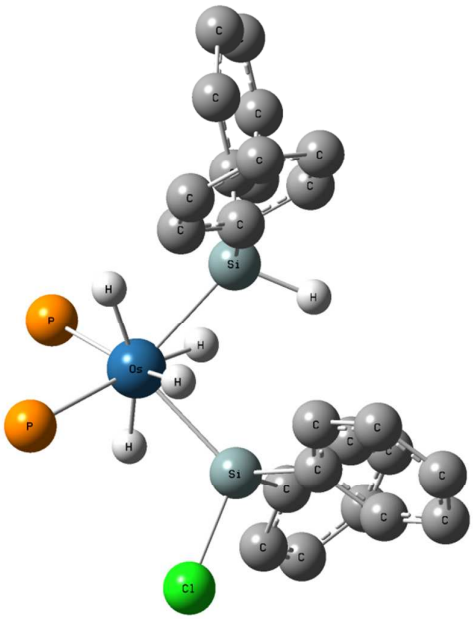

Si1-H = 1.48385
Si1-H1 = 2.23078
Si1-H2 = 2.45304
Si1-H4 = 2.15190

Si2-H2 = 2.30864
Si2-H3 = 2.16472
Si2-H4 = 2.54903

Os-H1 = 1.67407
Os-H2 = 1.62511
Os-H3 = 1.67264
Os-H4 = 1.63160

H1-H2 = 2.06795
H1-H4 = 2.70557
H2-H3 = 2.82373
H2-H4 = 2.67248
H3-H4 = 2.11836

Os-Si1 = 2.48777
Os-Si2 = 2.46239

Os-P1 = 2.53021
Os-P2 = 2.51764

P1-Os-P2 = 98.28272
Si1-Os-Si2 = 92.87440
Si1-Os-P1 = 106.14569
Si1-Os-P2 = 132.01671
Si2-Os-P1 = 130.31802
Si2-Os-P2 = 101.92702

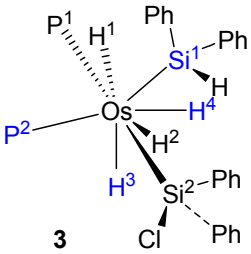

3

Figure S24. B3LYP optimized structure of complex **3**

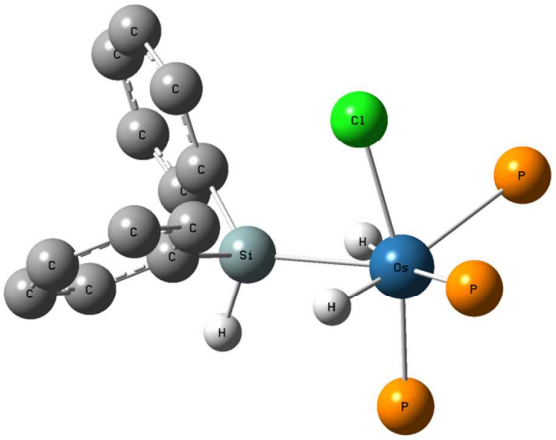

Os-P1 = 2.66633
Os-P2 = 2.56344
Os-P3 = 2.36934
Os-Si = 2.48018
Os-Cl = 2.51960
Os-H1 = 1.63115
Os-H2 = 1.61505

Cl-Si = 3.02250
Si-H = 1.48324
Si-H1 = 2.06037
Si-H2 = 2.18279
H1-H2 = 2.72328

P1-Os-P2 = 99.16524
Si-Os-P1 = 123.74652
Si-Os-P2 = 128.83680
Si-Os-P3 = 90.95010
P2-Os-P3 = 102.12419
P3-Os-P1 = 107.55139
H1-Os-P2 = 172.19775
H2-Os-P1 = 166.88645
Cl-Os-P3 = 165.24126

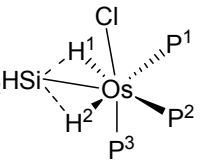

16

Figure S25. B3LYP optimized structure of complex **16**.

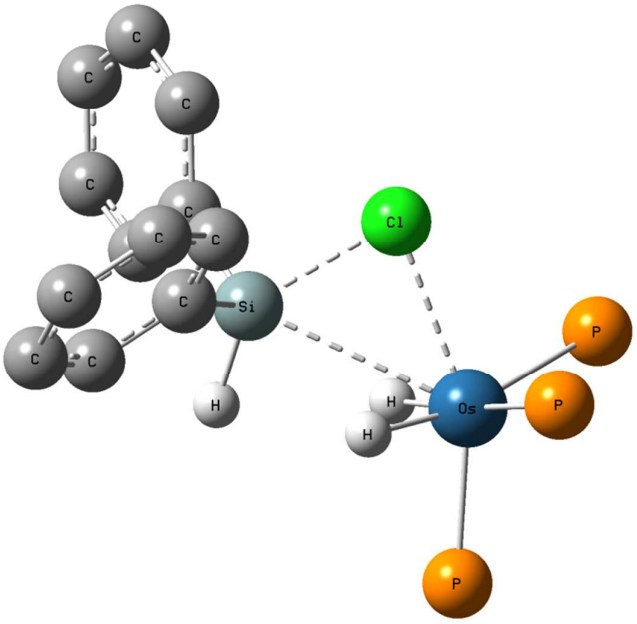

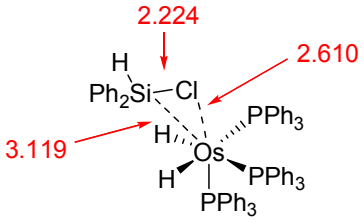

$TS_{16\text{-}16B}$

Figure S26. B3LYP optimized structure of **$TS_{16\text{-}16B}$**.

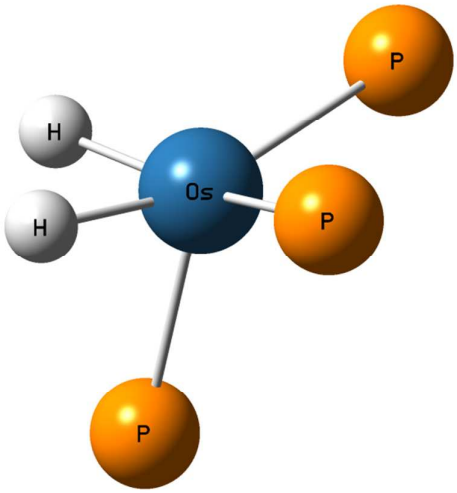

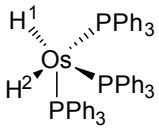

17
Os-H1 = 1.63845
Os-H2 = 1.64180
H1-H2 = 2.12337

H1-Os-H2 = 80.67941

Figure S27. B3LYP optimized structure of complex **17**.

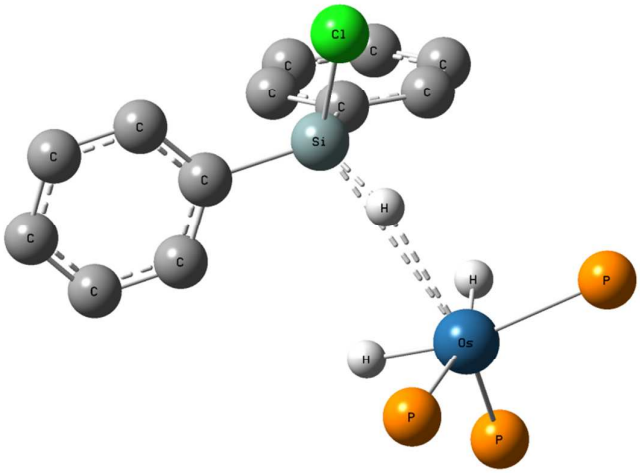

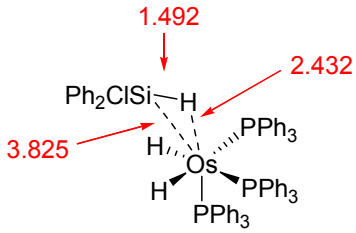

$TS_{17\text{-}2}$

Figure S28. B3LYP optimized structure of **$TS_{17\text{-}2}$**.

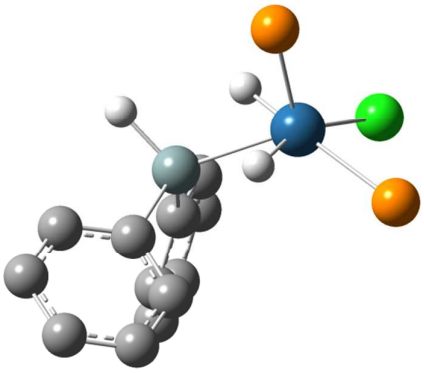

Os-P1 = 2.26407
Os-P2 = 2.53392

Os-Si = 2.41485
Os-Cl = 2.43679
Os-H1 = 1.61973
Os-H2 = 1.60855
Os-H = 3.32725

Cl-Si = 4.14507
Si-H = 1.48696
Si-H1 = 2.07012
Si-H2 = 2.29505
H1-H2 = 2.73462

P1-Os-P2 = 108.69571
Si-Os-P1 = 100.51449
Si-Os-P2 = 125.99279
Si-Os-Cl = 117.37882
H1-Os-P1 = 81.46661
H2-Os-P2 = 75.13185
Cl-Os-P1 = 117.57633
H1-Os-H2 = 115.79132

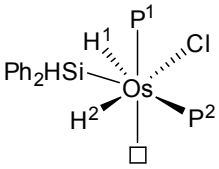

13

Figure S29. B3LYP optimized structure of complex **13**.

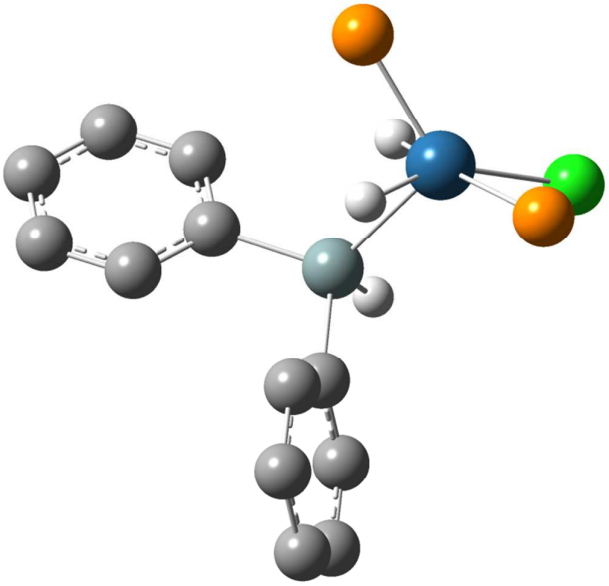

Os-P1 = 2.28713
Os-P2 = 2.55483

Os-Si = 2.40897
Os-Cl = 2.41773
Os-H1 = 1.61900
Os-H2 = 1.60852
Os-H = 3.17795

Cl-Si = 3.73392
Si-H = 1.48498
Si-H1 = 2.14277
Si-H2 = 2.34848
H1-H2 = 2.68030

P1-Os-P2 = 110.97868
Si-Os-P1 = 107.80588
Si-Os-P2 = 121.13876
Si-Os-Cl = 101.35585
H1-Os-P1 = 78.85672
H2-Os-P2 = 78.73702
Cl-Os-P1 = 129.27207
H1-Os-H2 = 112.28992

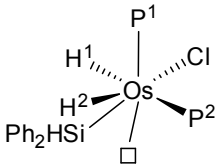

13A

Figure S30. B3LYP optimized structure of complex **13A**.

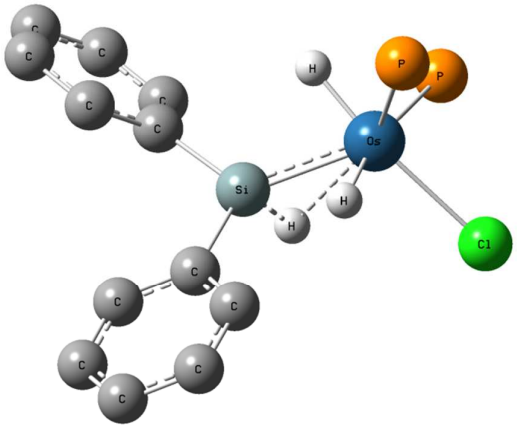

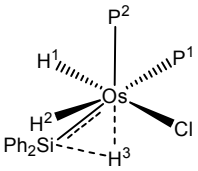

TS$_{13A-14}$

Os-H1 = 1.61302
Os-H2 = 1.61842
Os-H3 = 2.35183
Os-Si = 2.32391
Os-Cl = 2.49940
Si-Cl = 4.10929
Si-H2 = 2.15682
Si-H1 = 2.33251

Cl-Os-Si = 116.80534
Cl-Os-H2 = 80.25753
Cl-Os-H1 = 165.37155

P-Os-P = 107.55573
H3-Os-H2 = 82.49974
H1-Os-H2 = 114.04374

Figure S31. B3LYP optimized structure of complex **TS$_{13A-14}$**.

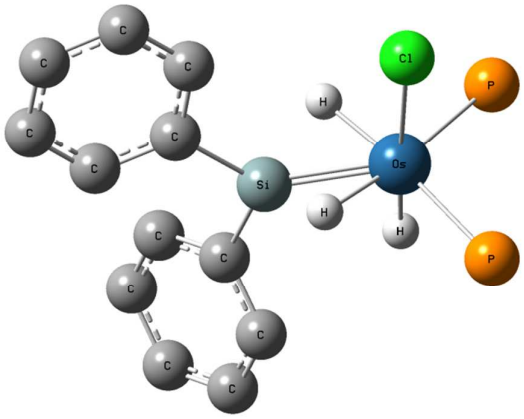

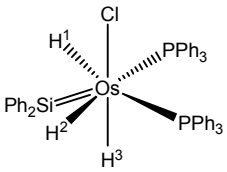

14

Os-H1= 1.75949
Os-H2 = 1.75995
Os-H3 = 1.61609
Os-Si = 2.25447
Os-Cl = 2.57951
Si-Cl = 3.83288
Si-H1 = 1.72046
Si-H2 = 1.71223
H2-H3 = 2.52980

Si-Os-Cl = 104.71547
P-Os-P = 101.94087
Cl-Os-H1 = 86.21975
H2-Os-H3 = 96.97456
H3-Os-Si = 78.44567
H1-Os-H2 = 90.24871

Figure S32. B3LYP optimized structure of complex **14**.

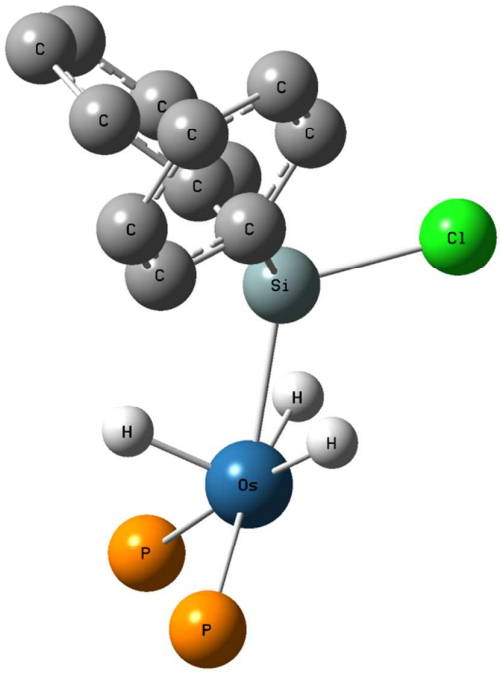

Os-P1 = 2.46405
Os-P2 = 2.43583

Os-Si = 2.37281
Os-H3 = 1.65101
Os-H1 = 1.64954
Os-H2 = 1.58103

Cl-Si = 2.14996
Si-H3 = 2.11686
Si-H1 = 2.01735
Si-H2 = 2.46368

H1-H2 = 2.54373
H2-H3 = 2.52829
H3-H1 = 2.50581

P1-Os-P2 = 104.32991
Si-Os-P1 = 121.35426
Si-Os-P2 = 126.59612

H2-Os-P1 = 84.03235
H3-Os-P2 = 77.81731
H3-Os-P1 = 172.92550
H1-Os-H2 = 103.86523

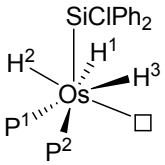

15

Figure S33. B3LYP optimized structure of complex **15**.

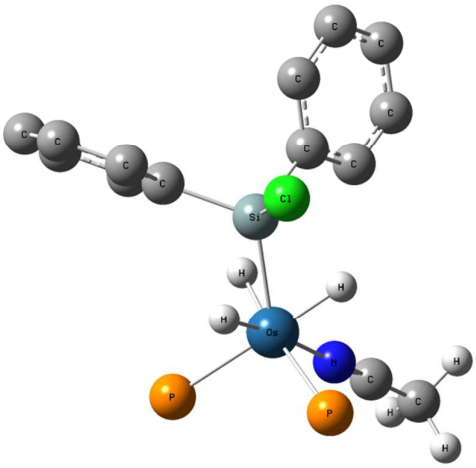

Os-P1 = 2.46695
Os-P2 = 2.44794
Os-Si = 2.36982
Os-N = 2.08998

Os-H1 = 1.64786
Os-H2 = 1.66176
Os-H3 = 1.63776

Cl-Si = 2.15584
Si-H1 = 2.15497
Si-H2 = 2.04580
Si-H3 = 2.17363

H1-H2 = 2.40476
H2-H3 = 2.54073
H1-H3 = 2.52615

P1-Os-P2 = 104.30287
Si-Os-P1 = 118.52389
Si-Os-P2 = 119.33689
Si-Os-N = 124.64144
H1-Os-P1 = 173.14377
H2-Os-P2 = 173.50102
H3-Os-N = 172.63315

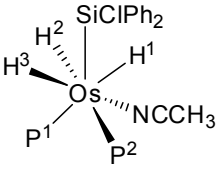

18

Figure S34. B3LYP optimized structure of complex **18**.